


CLINICAL RESEARCH ARTICLE OPEN



Investigating the influence of maternal prenatal BMI and perinatal depressive symptoms on neonatal brain network dynamics

Isabella L. C. Mariani Wigley^{1,2} , Alexandra Lautarescu^{3,4}, Elena Vartiainen^{1,2}, Elmo P. Pulli^{1,2}, Niloofar Hashempour^{1,2}, Harri Merisaari^{1,2}, Wajiha Bano^{1,2}, Silja Luotonen^{1,2,5}, Ashmeet Jolly^{1,2,6,7}, Ilkka Suuronen^{1,2}, Linnea Karlsson^{1,2,8,9}, Hasse Karlsson^{1,2,10}, Joana Cabral^{11,12}, Morten L. Kringelbach^{11,13,14}, Dafnis Batalle^{4,15}, A. David Edwards^{4,16} and Jetto J. Tuulari^{1,2,11,17}

© The Author(s) 2026

BACKGROUND: Elevated pre-pregnancy body mass index (BMI) and perinatal depressive symptoms have been linked to neonatal alterations in brain structure and function. This study examined associations between neonatal functional brain dynamics, maternal BMI, and perinatal depressive symptoms measured by the Edinburgh Postnatal Depression Scale (EPDS) in a community-based, largely low-risk cohort.

METHODS: Functional MRI and Leading Eigenvector Analysis (LEiDA) were applied in a neonatal cohort ($N = 437$; 236 males; mean gestational age 39.6 weeks) from the developing Human Connectome Project. We assessed whether neonatal brain-state probabilities related to maternal BMI and EPDS scores ($M = 5.6$, $SD = 4.3$), testing main effects and, separately, their interaction. The sample included 291 healthy-weight (BMI < 25), 98 overweight (25 BMI < 30), and 48 obese (BMI 30) mothers.

RESULTS: EPDS scores were low in this cohort and did not demonstrate associations with brain states or a significant BMI \times EPDS interaction. Higher maternal pre-pregnancy BMI was negatively associated with the stability of a functional network encompassing superior frontal, superior parietal, and temporal regions ($\beta = -0.129$, $p = 0.006$).

CONCLUSION: As this network is normally recruited more with age, reduced stability suggests slowed maturation of fronto-parieto-temporal systems and may signal early risk for later behavioral challenges.

Pediatric Research; <https://doi.org/10.1038/s41390-025-04726-2>

IMPACT:

- Higher maternal pre-pregnancy BMI is associated with reduced stability in a neonatal frontoparietal brain state, characterized by coordinated activity in frontal, parietal, and temporal regions.
- This state is one of six distinct dynamic connectivity patterns identified, reflecting core neonatal resting-state networks.
- The association was robust across multiple analytic models and clustering solutions.
- No significant effects were found for maternal depressive symptoms.
- These findings underscore the selective impact of maternal metabolic health on early brain organization, suggesting prenatal influences on the functional architecture of the newborn brain that may shape long-term neurodevelopmental trajectories.

INTRODUCTION

Researchers have long been intrigued by the complex relationship between maternal well-being during pregnancy and its potentially profound implications for fetal health and long-term outcomes.¹ Guided by the principles of the Developmental Origins of Health and Disease and Fetal Programming, our understanding of how prenatal environments shape future health trajectories has advanced considerably.^{2,3} These theories suggest that environmental exposure during critical periods of fetal development can have lasting effects on various physiological systems, including brain development, influencing disease risk later in life.

In this context, maternal physical well-being during pregnancy, and in particular overweight and obesity, have been associated with long-term neurodevelopmental outcomes in children with research suggesting that they may impact offspring brain development in utero. Previous studies have highlighted both structural and functional alterations in infants born to overweight mothers, as well as BMI-related neural phenotypes.^{4–6} For instance, one study found that higher maternal prepregnancy BMI relates to lower cortical thickness in key regions of the frontal lobe (i.e., left pars opercularis gyrus, left pars triangularis gyrus, and left rostral middle frontal gyrus).⁷ Moreover, changes in

A full list of author affiliations appears at the end of the paper.

Received: 16 June 2025 Revised: 1 December 2025 Accepted: 10 December 2025

Published online: 15 January 2026

functional connectivity associated with reward processing and cognitive control, like those observed in obese adults, were also found in 2-week-old infants born to mothers with high BMI.^{8,9} Infants born to healthy-weight mothers showed a greater recruitment of the dorsal anterior cingulate cortex regions into the prefrontal network compared to infants born to overweight mothers; functional connectivity strength in the dorsal anterior cingulate cortex was negatively correlated with maternal fat mass percentage measured in early pregnancy.⁸ This evidence suggests that exposure to maternal obesity in utero may be linked to changes in resting-state functional connectivity in newborns.

Beyond weight, other aspects of maternal well-being during pregnancy may influence offspring brain development. For instance, depressive symptoms during pregnancy have been linked to poorer neurobehavioral outcomes in children as well as alterations in brain structure and function.^{10–12} Those include, in neonates born to mothers with higher levels of prenatal depressive symptoms, altered diffusion properties in the amygdala,¹³ increased diffusivity in right frontal regions,¹⁴ decreased structural connectivity between the right amygdala and the right ventral prefrontal cortex,¹⁵ and increased functional connectivity of the amygdala with the left temporal cortex and insula, the bilateral anterior cingulate, medial orbitofrontal, and ventromedial prefrontal cortices.¹⁶ As evident from the above, numerous studies have investigated the link between exposure to maternal perinatal depressive symptoms and brain development in children. However, the specific brain regions involved and the direction of these associations remain inconsistent. Models of dynamic functional connectivity, which characterize functional networks over time, could help elucidate these effects by providing new insights into how maternal depressive symptoms alter neural development and connectivity patterns in the fetal brain under suboptimal conditions. Indeed, a recent study using resting-state functional magnetic resonance imaging (rs-fMRI) and a small sample of 20 neonates reported an association between maternal prenatal distress and the stability of a fronto-parietal brain network.¹⁷

Rs-fMRI is a widely used technique for investigating the interactions between brain regions and mapping comprehensive whole-brain functional connectivity networks. Brain connectivity is inherently dynamic and characterized by non-stationarity, with several models of dynamic functional connectivity (dFC) proposed to capture this variability.¹⁸ These methods track the real-time neural adjustments needed to regulate various brain states, adapt to transient conditions, and integrate information in order to study the formation, interaction, and dissolution of these network configurations over time.¹⁹ While the sliding window approach has been the most common method for evaluating dFC,²⁰ other methods with higher temporal resolution are gaining recognition for their ability to produce relevant and meaningful results. These methods include co-activation pattern analysis²¹ and phase-coherence pattern analysis.²² The former examines frames where regional activity exceeds a certain threshold, while the latter focuses on phase-locked synchronization of fMRI signal fluctuations. Specifically, a method called Leading Eigenvector Dynamics Analysis (LEiDA²²), which detects recurrent modes of phase coupling in fMRI signals, has identified subsystems that closely match functional networks reported in the literature, such as the default mode (DMN), limbic, dorsal attention (DAT), ventral attention (VAT), frontoparietal (FP), sensorimotor (SMT) and visual (VIS) networks.²³

LEiDA can detect brain activation patterns with high temporal precision, unlike correlation-based measures of functional connectivity. At each time point, the phase relationships between N brain regions are captured by a single vector of size $1 \times N$, effectively circumventing many limitations of alternative methods such as the sliding-window approach, which can amplify spurious

variations and lacks consensus on optimal window parameters, particularly in infant data.²⁴ LEiDA has revealed functional brain states that strongly overlap with canonical “resting-state networks” or “intrinsic connectivity networks” in adults.^{19,23,25} To our knowledge, LEiDA has also been applied to infant fMRI data twice^{17,26} and to early adolescent data once,²⁷ revealing meaningful networks and suggesting that these patterns can be reliably detected across human developmental stages. Specifically, in adults, the occurrence of dynamic functional networks characterized with LEiDA has been linked to cognitive performance,²² depressive history,²⁸ effects of psychoactive drugs,²³ and emotional reward task scores,²⁹ among others. In the neonatal context, recent evidence indicates that, at birth, the human brain already exhibits a dynamic connectivity landscape that is sensitive to age at scan.²⁶ Moreover, preterm-born infants show atypical dynamic connectivity patterns compared with term-born peers, which are associated with social, sensory processing, and repetitive behaviors at 18 months of age.²⁶ In light of this evidence, while it is increasingly recognized that maternal health conditions during pregnancy can influence infant developmental trajectories, the dynamic properties of the neonatal brain exposed to these prenatal influences remain unknown. Specifically, it is unclear how maternal well-being, encompassing both physical and mental health, may affect dFC in neonates.³⁰ While there are studies exploring maternal BMI and mental health separately in relation to early brain development, few have examined both factors together, despite their common interconnection.

In the current study, we analyzed rs-fMRI data from 437 mother-infant dyads, stemming from the developing Human Connectome Project (dHCP), applying the LEiDA method.²² Based on our previous study,¹⁷ we hypothesized that maternal BMI and depressive symptoms would be associated with the dynamics of these networks in the offspring. Our primary goal was to test the specific effects of each predictor separately while accounting for relevant covariates, and to explore potential interactions between BMI and depressive symptoms. Given the exploratory nature of this study, we did not specify directional hypotheses; rather, our analyses were designed to be hypothesis-generating, aimed at identifying potential associations that could inform future research.

METHODS

We used preprocessed data released as part of the dHCP data release 3.0, and the methods are previously described in detail.²⁶ We have kept the methods description similar to this prior report for consistency.²⁶

Participants

The infants were enrolled in the dHCP study between March 2015 and March 2021. Ethical approval was granted by the National Research Ethics Committee (14/LO/1169) and written informed consent was obtained from the parents of all participants before data collection began. Participants were invited to undergo fetal MRI scan, neonatal MRI scan, or both. This study focuses on data from neonatal functional magnetic resonance imaging (fMRI), which, at the time of analysis, included data from $n = 714$ scans. Participants were excluded for the following reasons: repeat scans, lack of completed EPDS, non-singleton pregnancies, missing or incomplete fMRI data, failure to pass the dHCP image quality control (<https://biomedica.github.io/dHCP-releasenotes/qc.html>), gestational age (GA) at birth below 32 weeks, infant’s postmenstrual age (PMA) at scan below 37 weeks, major incidental findings identified by a pediatric neuroradiologist (e.g., arterial ischemic infarcts, brain size <1st centile), failed visual image quality control, and the absence of a successful T2-weighted scan. The final sample for the MRI analysis consisted of $n = 437$ mother-infant dyads. For each mother–infant dyad, sociodemographic characteristics and medical history were collected at enrollment through parent-report questionnaires and review of medical records (Table 1). Additional maternal variables, including mental health history and use of alcohol, tobacco, and medications during pregnancy, are presented in

Table 1. Descriptive statistics and frequencies for key maternal and infant variables.

Variable	N	Mean	SD	Median	Min	Max
GA at birth	437	39.63	1.84	40.00	32.14	42.71
PMA at scan	437	41.36	1.69	41.43	37.00	44.71
Head Circumference at scan	437	33.77	7.20	35.00	33.77	39.50
Infant Sex [female count] (%)	437	201 (46.0%)	–	–	–	–
Motion during scan	437	53.61	67.4	24	0	365
Maternal age	437	33.78	4.66	34.00	17.00	46.00
Maternal BMI	437	24.26	4.60	24.26	16.87	43.55
Maternal gestational diabetes [yes] (%)	437	23 (5.3%)	–	–	–	–
Maternal education	427	23.33	4.45	23.00	14.00	41.00
Maternal EPDS	437	5.57	4.30	5.00	0.00	28.00

Maternal education is represented as the mother's age at the time she last attended continuous full-time education. This measure is an indirect proxy for attainment, as the same age may reflect different qualification levels.

GA at birth gestational age, PMA at scan postmenstrual age, Motion during scan number of outlier volumes based on DVARS interquartile range, Maternal BMI maternal pre-pregnancy body mass index, Maternal EPDS maternal perinatal depressive symptoms.

Table S1. Figure S1 shows EPDS distribution in mothers with and without a history of poor mental health.

MR image acquisition

The MR imaging was carried out using a 3T Philips Achieva scanner running modified Release 3.2.2 software. The length of the fMRI acquisition was 15 min and was collected with parameters: TE/TR = 38/392 ms, 2300 volumes, with an acquired spatial resolution of 2.15 mm isotropic voxels.³¹ To overcome challenges involved with non-sedated brain imaging of neonates, Neonatal Brain Imaging System (NBIS) was developed, consisting of a dedicated 32-channel array coil and a positioning device.³¹ The use of NBIS alongside advanced techniques for minimizing scan repeats and disturbance to the sleeping neonate has been demonstrated to improve signal-to-noise ratio 2.4 times compared to the use of an adult coil and ensure a 90% completion rate of the scan protocol.³²

Functional data preprocessing

The fMRI data were preprocessed using a neonatal imaging pipeline specifically optimized for the dHCP, as described in Fitzgibbon et al.³³ Briefly, each subject underwent corrections for susceptibility dynamic distortion and both intra- and intervolumetric motion using a customized pipeline that included slice-to-volume and rigid-body registration.^{34–37} To mitigate signal artifacts caused by head motion, cardiorespiratory fluctuations, and multiband acquisition,³⁸ 24 extended rigid-body motion parameters were regressed along with noise components identified through single-subject ICA using the FSL FIX tool (Oxford Centre for Functional Magnetic Resonance Imaging of the Brain's Software Library, version 5.0). The denoised data were aligned to T2-weighted native space via boundary-based registration³⁹ and then non-linearly registered to a standard space using a weekly template from the dHCP volumetric atlas,⁴⁰ employing a diffeomorphic multimodal (T1/T2) registration method.⁴¹ We defined the timeseries for fMRI data for each participant, using the same data and procedures as in previous research.²⁶ Each subject's T2-weighted volume was parcellated into 90 cortical and subcortical regions according to the AAL (i.e., Automated Anatomical Labeling) atlas,⁴² adapted for the neonatal brain,⁴³ and then manually corrected using the dHCP high-resolution template.⁴⁰ We mapped the AAL atlas into each subject's native space through non-linear registration utilizing a diffeomorphic symmetric normalization method (SyN),⁴⁴ applying it to T2-weighted images and previous segmentations. Gray matter segmentation and parcels were then transformed from T2 native space to fMRI space using a boundary-based linear registration method within the functional dHCP processing pipeline.³³ Finally, average timeseries were extracted for each of the 90 cortical and subcortical AAL areas. We employed FSL's 'fsl_motion_outliers' to detect volumes where DVARS (the root mean square intensity difference between consecutive volumes) exceeded 1.5 times the interquartile range (IQR) above the 75th percentile, following motion and distortion correction.⁴⁵ These volumes were flagged as motion outliers. The count of these motion-outlier volumes for each subject was documented and later used as a covariate in statistical analyses.

Temporal alterations in brain networks

We ran all the modeling in MATLAB 2022. Before running LEiDA, we first obtained the average fMRI signals from 90 cortical and subcortical areas defined by the UNC neonate AAL atlas using FSL fslmeants.⁴⁶ The time courses were bandpass filtered (0.02–0.10 Hz), the analytic phase was obtained using the Hilbert transform, and the leading eigenvectors of the phase coherence matrices were calculated at each time point.²² The eigenvectors were then clustered via K-means clustering using cosine distance with 200 replicates. For this exploratory study, the number of clusters (K) was varied between 2 and 10, based on previous studies suggesting that the optimal number of intrinsic networks is typically between 3 and 8.^{17,23,25,27} Clustering yields K states of brain activity, each representing a recurrent pattern of functional connectivity that can be characterized using measures derived from LEiDA.²² Specifically, we considered: (i) probability of occurrence, the proportion of time spent in each state, reflecting its dominance; (ii) lifetime, the mean duration a state persists once entered, indexing stability; and (iii) transitions, the likelihood of switching between states, reflecting network flexibility. In the present study, we examined associations between maternal pre-pregnancy BMI and perinatal depressive symptoms with the probability of occurrence and transitions of the identified brain states, as these measures are particularly informative about state dominance (i.e., probability of occurrence) and dynamic shifts (i.e., transitions). For completeness, lifetimes and full transition probability matrices are reported in the Supplementary Material (Figs. S3 and S4).

Maternal depressive symptoms

Maternal depressive symptoms were assessed using the EPDS⁴⁷ at each study visit. The EPDS is a 10-item questionnaire with a total score ranging from 0 to 30. Scores from the EPDS were included in the analysis if they were obtained during pregnancy (e.g., during a fetal scan visit) or in the early postnatal period (e.g., at the first neonatal scan), as these instances are indicative of mood during the prenatal and early postnatal phases. As the EPDS only asks about symptoms over the last 7 days, in cases where participants completed more than one EPDS questionnaire, the highest score was chosen. EPDS scores in our sample were available as follows: $n = 60$ only prenatal timepoints, $n = 362$ only postnatal timepoint, $n = 15$ both prenatal and postnatal timepoints. For prenatal assessments, the median GA was 30.4 weeks, with a range from 22.5 to 41.6 weeks. For postnatal assessment, the median PMA was 41.2 weeks, with a range from 33.1 to 44.7 weeks.

Statistical analysis

Analyses were performed using the statistical software R.⁴⁸ First, we tested the associations between LEiDA-derived network probabilities of occurrence (extracted from MATLAB into conventional tabular data) and maternal BMI during pregnancy, as well as maternal perinatal depressive symptoms, using General Linear Models (GLMs). We then performed another series of GLMs to test the associations between LEiDA-derived network transitions, maternal BMI during pregnancy, and perinatal

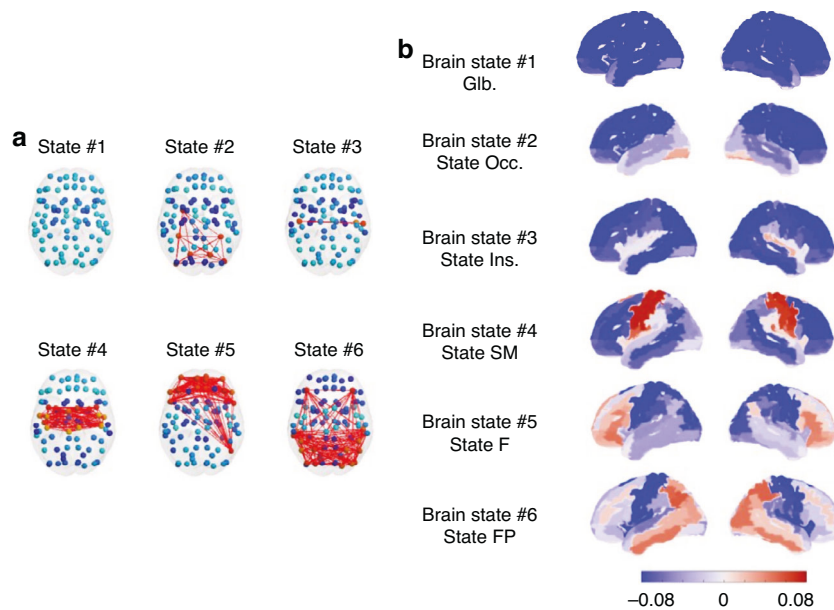


Fig. 1 Neonatal brain states identified with LEiDA ($K = 6$). Brain states are visualised in **a** showing red links between the brain areas that temporarily align their phase to another direction with respect to other brain areas, and **b** cortical representation coloring these areas in red, with the scale representing the cosine of their phase difference such that $\cos(0) = 1$ represents in-phase synchrony, while -1 (blue) represents a phase difference of 180° . Glb global, Occ occipital, Ins insula, SM sensorimotor, F frontal, FP frontoparietal.

depressive symptoms. Covariates were chosen based on previous literature and include infants' PMA at scan, sex, motion during scan, maternal age and gestational diabetes. For completeness, in the supplementary material, we report the results of the same models regarding the lifetime of brain networks (Fig. S11). Bivariate correlations between covariates and variables of interest are also reported in Supplementary Material, Section 3 (Figs. S5, S6, S7). To account for multiple comparisons, we applied the Bonferroni correction to the statistical tests based on the number of clusters, that is, for each independent hypothesis tested within each clustering solution. We reported uncorrected and Bonferroni corrected p values. Finally, we performed a sensitivity analysis excluding preterm infants ($N = 33$) and then including GA at birth, maternal medication use (Table S1) and smoking ($N = 11$) during pregnancy as covariates to assess their potential influence on results.

RESULTS

Neonatal brain states

Consistent with prior studies on infants, we set the K-means clustering solution with $K = 6$ distinct brain states for the main analyses (Fig. 1).^{17,26} In line with a previous study in infants that used an overlapping sample,²⁶ we identified a brain state of global signal coherence #1 (Glb. State), and five brain states that exhibited spatial patterns that resemble neonatal resting state networks⁴⁹: brain state #2 (Occipital State) was characterized by synchronous activity in the occipital cortex, brain state #3 (Insular State) encompassed the bilateral insulae, brain state #4 (SM State) showed synchrony in the bilateral sensorimotor cortices, brain state #5 (F State) in frontal areas and brain state #6 in the frontal cortex, angular gyrus, and posterior cingulate gyrus, which we refer to as the frontoparietal state (FP State) for simplicity. The repertoire of states obtained with varying the number of clusters between $K = 2$ to $K = 10$ is reported in Supplementary Material (Fig. S2).

Association between maternal prenatal BMI and perinatal EPDS with brain state probability of occurrence

Maternal pre-pregnancy BMI was negatively associated with the probability of occurrence of the FP functional network (i.e., brain state #6), which encompasses the superior frontal, superior parietal, and temporal brain regions ($\beta = -0.129$, $p = 0.006$)

(Fig. 2). While this association had a modest effect size, it remained robust after adjusting for covariates (i.e., infant's PMA at scan, sex, motion during scan, maternal age, and gestational diabetes, Table 2) and survived Bonferroni correction ($p_{\text{Bonf}} = 0.036$). Notably, as the frontoparietal state (i.e., state #6) shows a consistent spatial configuration across higher clustering solutions ($K = 7, 8, 10$), we tested the association between pre-pregnancy BMI and its probability of occurrence also when K was set at 7, 8, and 10. We observed that this association remained consistently negative and statistically significant (Tables S4, S5, S6). The uncorrected and corrected p values for each brain state were as follows: brain state #7 for $K = 7$ ($\beta = -0.132$, $p = 0.006$, $p_{\text{Bonf}} = 0.041$); brain state #8 for $K = 8$ ($\beta = -0.130$, $p = 0.006$, $p_{\text{Bonf}} = 0.048$); and brain state #10 for $K = 10$ ($\beta = -0.133$, $p = 0.005$, $p_{\text{Bonf}} = 0.037$). Since our sample included preterm infants, we conducted a sensitivity analysis to test the robustness of our findings. The association between maternal pre-pregnancy BMI and the probability of occurrence of the FP network remained consistent when excluding $N = 33$ preterm infants ($\beta = -0.14$, $p = 0.006$, $p_{\text{Bonf}} = 0.045$; Table S7) and when including GA at birth as a covariate ($\beta = -0.14$, $p = 0.006$, $p_{\text{Bonf}} = 0.048$; Table S8). In the Supplementary Material (Section 5), we report sensitivity analyses including other relevant variables such as maternal use of medications (Table S9) and smoking during pregnancy ($N = 11$; Table S10), none of which altered the results. In the Supplementary Material we provided more details on the FP network (Fig. S8)—including specific brain regions based on the AAL atlas—the associations between maternal prepregnancy BMI and the probability of the occurrence of all brain states when $K = 6$ (Fig. S9), and the relationship between maternal pre-pregnancy BMI and the lifetime of brain states (Fig. S12).

Maternal perinatal depressive symptoms were not associated with the occurrence of any of the functional networks examined. Although beyond the primary scope of this study, we explored whether maternal pre-pregnancy BMI and depressive symptoms interact in shaping FP network occurrence. However, these results did not survive correction for multiple comparisons and are reported in the Supplementary Material (Fig. S10, Table S2; Fig. S11, Table S3).

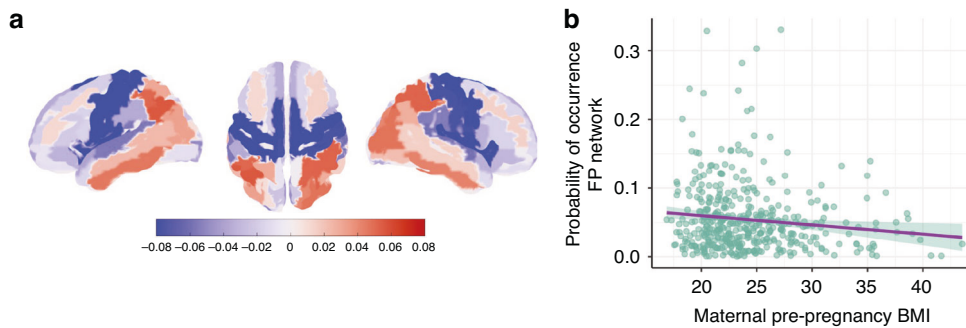


Fig. 2 Maternal pre-pregnancy BMI associates negatively with the probability of occurrence of a frontoparietal brain network in neonates. **a** Visualization of the network, and **b** scatter plot of the association. FP frontoparietal, BMI body mass index.

Table 2. Model results.

Term	Estimate	SE	<i>p</i>	<i>p</i> _{Bonf}
Maternal EPDS	0.0005	0.0005	0.370	1.00
Maternal BMI	-0.0014	0.0005	0.006	0.036
Maternal age	0.0001	0.0005	0.942	1.00
Gestational diabetes	-0.003	0.0104	0.738	1.00
Infant sex	0.0094	0.0046	0.042	0.294
Infant PMA at scan (weeks)	-0.0026	0.0014	0.064	0.449
Motion	0.0002	0.0003	<0.001	<0.001

The table includes standardized beta coefficients (Estimate), standard errors (SE), and *p* values. Adjusted *R*² for the model is 0.10. Maternal EPDS; Maternal perinatal depressive symptoms, Maternal BMI Maternal Body Mass Index, Infant PMA at scan; postmenstrual age at scan, Motion; infants motion during scan.

Association between maternal prenatal BMI and perinatal EPDS with brain state transitions

Figure 3 shows the associations between maternal pre-pregnancy BMI and brain state transitions. Higher maternal BMI was significantly associated with a reduced likelihood of transitioning from the occipital state #2 to the sensorimotor state #4 ($\beta = -0.135$, $p = 0.006$, $p_{\text{Bonf}} = 0.048$). Additional associations were observed but did not survive correction for multiple comparisons: higher BMI was related to a lower probability of transitioning from the sensorimotor state #4 to the frontoparietal state #6 ($\beta = -0.129$, $p = 0.008$, $p_{\text{Bonf}} = 0.064$), from the sensorimotor state #4 to insular state #3 ($\beta = -0.096$, $p = 0.045$, $p_{\text{Bonf}} = 0.384$), and from the sensorimotor state #4 to the frontal state #5 ($\beta = -0.101$, $p = 0.036$, $p_{\text{Bonf}} = 0.304$). In contrast, BMI was associated with an increased likelihood of transitioning from the frontoparietal state #6 to the global state A ($\beta = 0.125$, $p = 0.011$, $p_{\text{Bonf}} = 0.088$).

EPDS scores, were not associated with transitions of any of the functional networks examined.

DISCUSSION

Dynamic connectivity in the neonate brain

Our study describes that the human brain establishes a well-organized dynamic connectivity landscape in the brain soon after birth. Consistent with earlier research using both fMRI^{50,51} and EEG,⁵² we found that newborns spend a significant amount of time in a state of global phase synchrony. Whole-brain synchrony state 1 exhibited the greatest fractional occupancy, indicating a dominant pattern of whole-brain synchronization. The remaining five states strongly overlap with functional connectivity patterns previously identified in pediatric populations.^{53–55} Specifically, the second and fourth states were characterized by a strong

involvement of auditory, sensorimotor, and visual regions, aligning with evidence that sensory networks are among the first to emerge and are robustly expressed in infancy.^{45,56,57} In contrast, the third state was dominated by regions of the salience network,⁵⁸ notably the insula and anterior cingulate, which are detectable in infancy but undergo substantial refinement over development.⁵⁹ Finally, the fifth and sixth states involved dorsal attention and frontoparietal control networks,⁵⁸ which mature later in childhood, consistent with their lower probability of occurrence in our data. This consistency reinforces the findings of studies on dFC in newborns and underscores the importance of large-scale brain activity for early development.^{60,61} Such activity likely supports the emergence of widespread cortical networks and long-range connections that continue to mature throughout the first postnatal year, providing a foundation for sensory, motor, and higher-order cognitive functions.

Intergenerational implications of maternal overweight

We observed a negative association between the probability of occurrence of a functional network encompassing the superior frontal, superior parietal, and temporal regions and maternal pre-pregnancy BMI. This aligns with prior evidence that maternal metabolic health influences fetal brain development^{4–6,8,9,62–64} and highlights the particular sensitivity to this effect of frontal regions. Indeed, previous studies have linked different properties of infants' frontal regions to maternal BMI, reporting both reduced cortical thickness⁶² and altered static functional connectivity.^{5,6} Our dynamic modeling approach extends these findings by showing that higher maternal BMI is associated with reduced stability of fronto-parieto-temporal states. Since the FP network becomes increasingly prominent with postnatal age,²⁶ the reduced probability of occurrence observed here suggests delayed maturation of this system. Moreover, several regions within the FP network overlap with the anterior Default Mode Network (DMN),⁶⁵ which undergoes substantial reorganization in early life through progressive recruitment of frontal areas. The reduced occurrence of these regions in association with maternal BMI therefore reinforces the notion of delayed network development. These alterations also echo reports of atypical DMN patterns in overweight and obese adults,^{66–68} which have been linked to poorer cognitive outcomes later in life.^{67,68} Another indicator of the destabilizing effect of maternal weight on infant brain development is the finding that higher maternal pre-pregnancy BMI is associated with a reduced likelihood of transitions from the occipital to the sensorimotor state and from the sensorimotor to the frontal and fronto-parietal states. Typically, transitions from occipital to sensorimotor states support visuomotor development and sensory integration,⁶⁹ whereas transitions from sensorimotor to fronto-parietal states reflect the emerging maturation of higher-order networks. This developmental trajectory coincides with substantial interneuron migration into frontal and parietal regions,⁷⁰ in contrast to the relatively mature sensorimotor

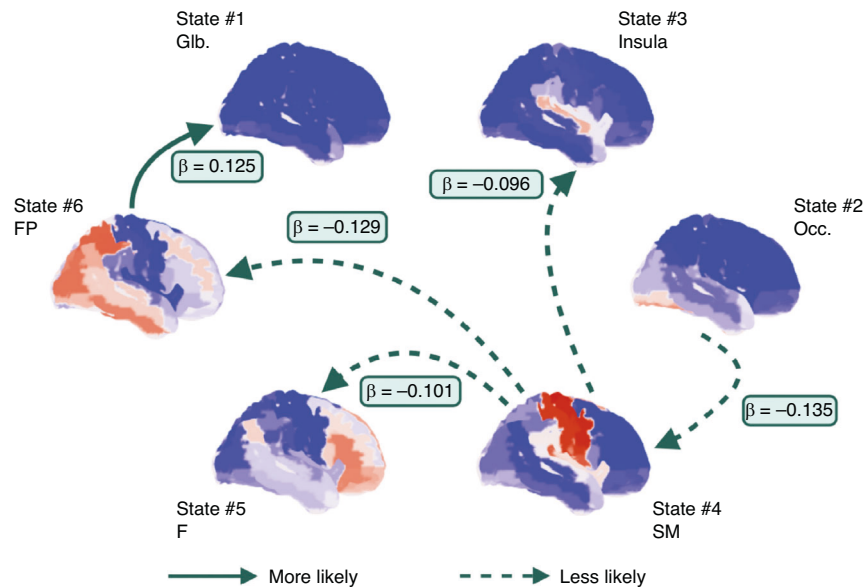


Fig. 3 Probability of transition and maternal pre-pregnancy BMI ($K = 6$). The probability of transition from state #2 to #4, from #4 to #3, from #4 to #5 and from #4 to #6 is negatively predicted by maternal pre-pregnancy BMI. The probability of transition from state #6 to global state A is positively predicted by maternal pre-pregnancy BMI. Glb global, Occ occipital, SM sensorimotor, F frontal, FP frontoparietal, BMI body mass index.

systems.⁷¹ Disruptions in these early transition patterns may compromise the integration of visuomotor and higher-order functions, helping to explain why children born to overweight or obese mothers often show deficits in motor coordination⁷² and suboptimal visuomotor skills.^{73,74} Critically, these very early alterations in network dynamics across occipital, sensorimotor, and fronto-parietal networks may set the stage for later atypical connectivity patterns in multiple brain systems. In adults, such atypical patterns have been linked to impairments in attention, working memory, executive and inhibitory control, and broader cognitive control dysfunction—a phenotype commonly observed in overweight and obese individuals that can contribute to dysregulated eating and energy imbalance.^{75–77} Taken together, the present findings suggest that the brain dynamics of neonates born to mothers with higher BMI already mirror patterns associated with later behavioral and cognitive challenges. Although we did not assess mechanisms directly, hormonal and inflammatory changes associated with maternal obesity have been proposed as potential contributors to these intergenerational effects, highlighting the impact of maternal metabolic health on early neurodevelopment.

Limitations and future directions

While this study provides valuable insights, some limitations must be considered. First, our study is cross-sectional and thus does not allow for causal inference. Second, the scale of depressive symptoms is unable to capture the potential mediating biological or physiological mechanisms. Furthermore, EPDS only captures symptoms in the last 7 days; this narrow window may not fully reflect mental health throughout the perinatal period, as scores could be influenced by transient fluctuations. In addition, very few participants with high EPDS scores could have affected associations between maternal perinatal depressive symptoms and neonatal brain connectivity. Third, although BMI is a well-established measure of weight status, it does not directly measure metabolic health, and we were unable to take into account changes in weight during pregnancy. It should also be mentioned that BMI does not distinguish between fat and muscle mass, which means that people with high muscle mass may have a higher BMI despite having low body fat.⁷⁸ Fourth, motion during

scanning was a significant covariate in our analyses, and although we adjusted for it statistically, its influence represents a potential limitation. Finally, although the dHCP includes longitudinal developmental outcome data, linking neonatal brain dynamics to later behavioral or cognitive trajectories was beyond the scope of the present study and should be addressed in future work. Future research incorporating longitudinal designs and objective measures of biological processes, such as hormonal changes, inflammatory markers, and genetic factors, could provide deeper insight into the underlying mechanisms linking maternal mental health with early brain development in offspring.

DATA AVAILABILITY

The AAL-UNC atlas adapted to the dHCP template space, and pre-processed BOLD timeseries data generated in this study have been deposited in the Zenodo database under accession code <https://doi.org/10.5281/zenodo.7053984>. The fMRI datasets and clinical data are available under restricted access as per dHCP data release conditions, access can be obtained via <https://data.developingconnectome.org>. The corresponding author is responsible for submitting a competing interests statement on behalf of all authors of the paper. This statement must be included in the submitted article file.

REFERENCES

- Davis, E. P. & Narayan, A. J. Pregnancy as a period of risk, adaptation, and resilience for mothers and infants. *Dev. Psychopathol.* **32**, 1625–1639 (2020).
- Gluckman, P. D. & Hanson, M. A. The developmental origins of health and disease. in *Early Life Origins Health Disease* 1–7 (Springer, 2006).
- O'Donnell, K. J. & Meaney, M. J. Fetal origins of mental health: the developmental origins of health and disease hypothesis. *Am. J. Psychiatry* **174**, 319–328 (2017).
- Rosberg, A. et al. Associations between maternal pre-pregnancy BMI and infant striatal mean diffusivity. *BMC Med.* **22**, 140 (2024).
- Norr, M. E., Hect, J. L., Lenniger, C. J., Van den Heuvel, M. & Thomason, M. E. An examination of maternal prenatal BMI and human fetal brain development. *J. Child Psychol. Psychiatry* **62**, 458–469 (2021).
- Rajasilta, O. et al. Maternal pre-pregnancy BMI associates with neonate local and distal functional connectivity of the left superior frontal gyrus. *Sci. Rep.* **11**, 19182 (2021).
- Na, X. et al. Maternal obesity during pregnancy is associated with lower cortical thickness in the neonate brain. *Am. J. Neuroradiol.* **42**, 2238–2244 (2021).
- Li, X. et al. Differences in brain functional connectivity at resting state in neonates born to healthy obese or normal-weight mothers. *Int. J. Obes.* **40**, 1931–1934 (2016).

9. Salzwedel, A. P. et al. Maternal adiposity influences neonatal brain functional connectivity. *Front. Hum. Neurosci.* **12**, 514 (2019).
10. Meaney, M. J. Perinatal maternal depressive symptoms as an issue for population health. *Am. J. Psychiatry* **175**, 1084–1093 (2018).
11. Lautarescu, A., Craig, M. C. & Glover, V. Prenatal stress: effects on fetal and child brain development. *Int. Rev. Neurobiol.* **150**, 17–40 (2020).
12. Mandl, S. et al. The effect of prenatal maternal distress on offspring brain development: a systematic review. *Early Hum. Dev.* **192**, 106009 (2024).
13. Rifkin-Graboi, A. et al. Prenatal maternal depression associates with microstructure of right amygdala in neonates at birth. *Biol. Psychiatry* **74**, 837–844 (2013).
14. Posner, J. et al. Alterations in amygdala–prefrontal circuits in infants exposed to prenatal maternal depression. *Transl. Psychiatry* **6**, e935–e935 (2016).
15. Dean, D. C. et al. Association of prenatal maternal depression and anxiety symptoms with infant white matter microstructure. *JAMA Pediatr.* **172**, 973–981 (2018).
16. Qiu, A. et al. Prenatal maternal depression alters amygdala functional connectivity in 6-month-old infants. *Transl. Psychiatry* **5**, e508–e508 (2015).
17. Tuulari, J. J. et al. Maternal prenatal distress exposure negatively associates with the stability of neonatal frontoparietal network. *Stress* **27**, 2275207 (2024).
18. Preti, M. G., Bolton, T. A. & Van De Ville, D. The dynamic functional connectome: state-of-the-art and perspectives. *Neuroimage* **160**, 41–54 (2017).
19. Vohryzek, J., Deco, G., Cessac, B., Kringelbach, M. L. & Cabral, J. Ghost attractors in spontaneous brain activity: recurrent excursions into functionally-relevant bold phase-locking states. *Front. Syst. Neurosci.* **14**, 20 (2020).
20. Sakoglu, Ü et al. A method for evaluating dynamic functional network connectivity and task-modulation: application to schizophrenia. *Magn. Reson. Mater. Phys., Biol. Med.* **23**, 351–366 (2010).
21. Karahanoglu, F. I. & Van De Ville, D. Transient brain activity disentangles fMRI resting-state dynamics in terms of spatially and temporally overlapping networks. *Nat. Commun.* **6**, 7751 (2015).
22. Cabral, J. et al. Cognitive performance in healthy older adults relates to spontaneous switching between states of functional connectivity during rest. *Sci. Rep.* **7**, 5135 (2017).
23. Lord, L.-D. et al. Dynamical exploration of the repertoire of brain networks at rest is modulated by psilocybin. *Neuroimage* **199**, 127–142 (2019).
24. Leonardi, N. & Van De Ville, D. On spurious and real fluctuations of dynamic functional connectivity during rest. *Neuroimage* **104**, 430–436 (2015).
25. Cahart, M.-S. et al. Test-retest reliability of time-varying patterns of brain activity across single band and multiband resting-state functional magnetic resonance imaging in healthy older adults. *Front. Hum. Neurosci.* **16**, 980280 (2022).
26. França, L. G. et al. Neonatal brain dynamic functional connectivity in term and preterm infants and its association with early childhood neurodevelopment. *Nat. Commun.* **15**, 16 (2024).
27. Fasano, M. C. et al. The early adolescent brain on music: analysis of functional dynamics reveals engagement of orbitofrontal cortex reward system. *Hum. Brain Mapp.* **44**, 429–446 (2023).
28. Figueroa, C. A. et al. Altered ability to access a clinically relevant control network in patients remitted from major depressive disorder. *Hum. Brain Mapp.* **40**, 2771–2786 (2019).
29. Stark, E. A. et al. The power of smiling: the adult brain networks underlying learned infant emotionality. *Cereb. Cortex* **30**, 2019–2029 (2020).
30. Pulli, E. P. et al. Prenatal exposures and infant brain: review of magnetic resonance imaging studies and a population description analysis. *Hum. Brain Mapp.* **40**, 1987–2000 (2019).
31. Edwards, A. D. et al. The developing human connectome project neonatal data release. *Front. Neurosci.* **16**, 886772 (2022).
32. Hughes, E. J. et al. A dedicated neonatal brain imaging system. *Magn. Reson. Med.* **78**, 794–804 (2017).
33. Fitzgibbon, S. P. et al. The developing human connectome project (DHCP) automated resting-state functional processing framework for newborn infants. *Neuroimage* **223**, 117303 (2020).
34. Andersson, J. L., Graham, M. S., Drobnyak, I., Zhang, H. & Campbell, J. Susceptibility-induced distortion that varies due to motion: correction in diffusion MR without acquiring additional data. *Neuroimage* **171**, 277–295 (2018).
35. Andersson, J. L. et al. Towards a comprehensive framework for movement and distortion correction of diffusion MR images: within volume movement. *Neuroimage* **152**, 450–466 (2017).
36. Andersson, J. L., Hutton, C., Ashburner, J., Turner, R. & Friston, K. Modeling geometric deformations in EPI time series. *Neuroimage* **13**, 903–919 (2001).
37. Andersson, J. L., Skare, S. & Ashburner, J. How to correct susceptibility distortions in spin-echo echo-planar images: application to diffusion tensor imaging. *Neuroimage* **20**, 870–888 (2003).
38. Salimi-Khorshidi, G. et al. Automatic denoising of functional MRI data: combining independent component analysis and hierarchical fusion of classifiers. *Neuroimage* **90**, 449–468 (2014).
39. Greve, D. N. & Fischl, B. Accurate and robust brain image alignment using boundary-based registration. *Neuroimage* **48**, 63–72 (2009).
40. Schuh, A. et al. Unbiased construction of a temporally consistent morphological atlas of neonatal brain development. *BioRxiv* <https://doi.org/10.1101/251512> (2018).
41. Avants, B. B., Epstein, C. L., Grossman, M. & Gee, J. C. Symmetric diffeomorphic image registration with cross-correlation: evaluating automated labeling of elderly and neurodegenerative brain. *Med. Image Anal.* **12**, 26–41 (2008).
42. Tzourio-Mazoyer, N. et al. Automated anatomical labeling of activations in SPM using a macroscopic anatomical parcellation of the MNI MRI single-subject brain. *Neuroimage* **15**, 273–289 (2002).
43. Shi, F. et al. Infant brain atlases from neonates to 1- and 2-year-olds. *PLoS one* **6**, e18746 (2011).
44. Avants, B. B. et al. A reproducible evaluation of ants similarity metric performance in brain image registration. *Neuroimage* **54**, 2033–2044 (2011).
45. Eyre, M. et al. The developing human connectome project: typical and disrupted perinatal functional connectivity. *Brain* **144**, 2199–2213 (2021).
46. Jenkinson, M., Beckmann, C. F., Behrens, T. E., Woolrich, M. W. & Smith, S. M. Fsl. *Neuroimage* **62**, 782–790 (2012).
47. Cox, J. L., Holden, J. M. & Sagovsky, R. Detection of postnatal depression: development of the 10-item edinburgh postnatal depression scale. *Br. J. Psychiatry* **150**, 782–786 (1987).
48. R Core Team. R: A language and environment for statistical computing. (2024).
49. De Asis-Cruz, J., Bouyssi-Kobar, M., Evangelou, I., Vezina, G. & Limperopoulos, C. Functional properties of resting state networks in healthy full-term newborns. *Sci. Rep.* **5**, 17755 (2015).
50. Ma, X., Wu, X. & Shi, Y. Changes of dynamic functional connectivity associated with maturity in late preterm infants. *Front. Pediatr.* **8**, 412 (2020).
51. Wen, X. et al. Development of dynamic functional architecture during early infancy. *Cereb. Cortex* **30**, 5626–5638 (2020).
52. Tokariev, A. et al. Large-scale brain modes reorganize between infant sleep states and carry prognostic information for preterms. *Nat. Commun.* **10**, 2619 (2019).
53. Kiviniemi, V. et al. Slow vasomotor fluctuation in fmri of anesthetized child brain. *Magn. Reson. Med.* **44**, 373–378 (2000).
54. Fransson, P. et al. Resting-state networks in the infant brain. *Proc. Natl. Acad. Sci.* **104**, 15531–15536 (2007).
55. Fransson, P. et al. Spontaneous brain activity in the newborn brain during natural sleep—an fMRI study in infants born at full term. *Pediatr. Res.* **66**, 301–305 (2009).
56. Smyser, C. D. et al. Longitudinal analysis of neural network development in preterm infants. *Cereb. Cortex* **20**, 2852–2862 (2010).
57. Doria, V. et al. Emergence of resting state networks in the preterm human brain. *Proc. Natl. Acad. Sci.* **107**, 20015–20020 (2010).
58. Yeo, B. T. et al. The organization of the human cerebral cortex estimated by intrinsic functional connectivity. *J. Neurophysiol.* **106**, 1125–1165 (2011).
59. Power, J. D., Fair, D. A., Schlaggar, B. L. & Petersen, S. E. The development of human functional brain networks. *Neuron* **67**, 735–748 (2010).
60. Tau, G. Z. & Peterson, B. S. Normal development of brain circuits. *Neuropsychopharmacology* **35**, 147–168 (2010).
61. Damaraju, E. et al. Functional connectivity in the developing brain: a longitudinal study from 4 to 9 months of age. *Neuroimage* **84**, 169–180 (2014).
62. Na, X. et al. Maternal obesity during pregnancy is associated with lower cortical thickness in the neonate brain. *Am. J. Neuroradiol.* **42**, 2238 (2021).
63. Ou, X., Thakali, K. M., Shankar, K., Andres, A. & Badger, T. M. Maternal adiposity negatively influences infant brain white matter development. *Obesity* **23**, 1047–1054 (2015).
64. Spann, M. N. et al. Association of maternal prepregnancy body mass index with fetal growth and neonatal thalamic brain connectivity among adolescent and young women. *JAMA Netw. Open* **3**, e2024661–e2024661 (2020).
65. Buckner, R. L., Andrews-Hanna, J. R. & Schacter, D. L. The brain’s default network: anatomy, function, and relevance to disease. *Ann. N. Y. Acad. Sci.* **1124**, 1–38 (2008).
66. Tregellas, J. R. et al. Altered default network activity in obesity. *Obesity* **19**, 2316–2321 (2011).
67. Syan, S. K. et al. Deficits in executive function and suppression of default mode network in obesity. *Neuroimage: Clin.* **24**, 102015 (2019).
68. Xu, S. et al. Altered structural node of default mode network mediated general cognitive ability in young adults with obesity. *Prog. Neuro Psychopharmacol. Biol. Psychiatry* **135**, 111132 (2024).
69. Culham, J. C., Cavina-Pratesi, C. & Singhal, A. The role of parietal cortex in visuomotor control: what have we learned from neuroimaging?. *Neuropsychologia* **44**, 2668–2684 (2006).
70. Paredes, M. F. et al. Extensive migration of young neurons into the infant human frontal lobe. *Science* **354**, aaf7073 (2016).
71. Dall’Orso, S. et al. Development of functional organization within the sensorimotor network across the perinatal period. *Hum. Brain Mapp.* **43**, 2249–2261 (2022).

72. Hunt, K. J. et al. The association between maternal pre-pregnancy BMI, gestational weight gain and child adiposity: a racial-ethnically diverse cohort of children. *Pediatr. Obes.* **17**, e12911 (2022).
73. Adane, A., Mishra, G. & Tooth, L. Maternal preconception weight trajectories, pregnancy complications and offspring's childhood physical and cognitive development. *J. Dev. Orig. Heal. Dis.* **9**, 653–660 (2018).
74. Hinkle, S., Sharma, A., Kim, S. & Schieve, L. Maternal prepregnancy weight status and associations with children's development and disabilities at kindergarten. *Int. J. Obes.* **37**, 1344–1351 (2013).
75. Marek, S. & Dosenbach, N. U. The frontoparietal network: function, electrophysiology, and importance of individual precision mapping. *Dialogues Clin. Neurosci.* **20**, 133–140 (2018).
76. Guo, H., Han, J., Xiao, M. & Chen, H. Functional alterations in overweight/obesity: focusing on the reward and executive control network. *Rev. Neurosci.* **35**, 697–707 (2024).
77. Doucet, G. E., Rasgon, N., McEwen, B. S., Micali, N. & Frangou, S. Elevated body mass index is associated with increased integration and reduced cohesion of sensory-driven and internally guided resting-state functional brain networks. *Cereb. Cortex* **28**, 988–997 (2018).
78. Sweatt, K., Garvey, W. T. & Martins, C. Strengths and limitations of BMI in the diagnosis of obesity: What is the path forward?. *Curr. Obes. Rep.* **13**, 584–595 (2024).

AUTHOR CONTRIBUTIONS

Conceptualization: J.J.T., A.L.; methodology: J.J.T., D.B.; data analysis: I.L.C.M.W., D.B.; data acquisition: J.C., S.F., E.H., R.D., J.V.H., A.N.P., A.C., T.A.; interpretation of results: I.L.C.M.W., A.T., J.C., E.D., J.J.T.; funding acquisition: D.B., A.D.E., J.J.T.; project administration: D.B., A.D.E., J.J.T.; supervision: J.J.T.; writing—original draft: I.L.C.M.W.; writing—review and editing: All authors.

FUNDING

I.L.C.M.W. was supported by a postdoctoral fellowship from the Sigrid Juselius Foundation through J.J.T. fellowship. J.J.T. was supported by the Finnish Medical Foundation, the Emil Aaltonen Foundation, the Sigrid Juselius Foundation, the Signe and Ane Gyllenberg Foundation, the Hospital District of Southwest Finland State Research Grants, the Alfred Kordelin Foundation, the Juho Vainio Foundation and the Orion research Foundation. The Developing Human Connectome Project was supported by the European Research Council under the European Union's Seventh Framework Programme (FP7/20072013)/ERC grant agreement no. 319456 (dHCP project). D.B. received support from a Wellcome Trust Seed Award in Science [217316/Z/19/Z]. D.B. acknowledges structural funding by the NIHR Maudsley Biomedical Research Centre at South London and Maudsley NHS Foundation Trust and King's College London. The views expressed are those of the author(s) and not necessarily those of the NIHR or the Department of Health and Social Care. J.C. is

supported by the Portuguese Foundation for Science and Technology (FCT) through LARSyS funding (<https://doi.org/10.54499/LA/P/0083/2020>). E.P.P. is supported by the Signe and Ane Gyllenberg Foundation. The authors report no biomedical financial interests or potential conflicts of interest. Open Access funding provided by University of Turku (including Turku University Central Hospital).

COMPETING INTERESTS

The authors declare no competing interests.

CONSENT STATEMENT

Ethical approval was granted by the National Research Ethics Committee (14/LO/1169) and written informed consent was obtained from the parents of all participants before data collection began.

ADDITIONAL INFORMATION

Supplementary information The online version contains supplementary material available at <https://doi.org/10.1038/s41390-025-04726-2>.

Correspondence and requests for materials should be addressed to Isabella L. C. Mariani Wigley.

Reprints and permission information is available at <http://www.nature.com/reprints>

Publisher's note Springer Nature remains neutral with regard to jurisdictional claims in published maps and institutional affiliations.



Open Access This article is licensed under a Creative Commons Attribution 4.0 International License, which permits use, sharing, adaptation, distribution and reproduction in any medium or format, as long as you give appropriate credit to the original author(s) and the source, provide a link to the Creative Commons licence, and indicate if changes were made. The images or other third party material in this article are included in the article's Creative Commons licence, unless indicated otherwise in a credit line to the material. If material is not included in the article's Creative Commons licence and your intended use is not permitted by statutory regulation or exceeds the permitted use, you will need to obtain permission directly from the copyright holder. To view a copy of this licence, visit <http://creativecommons.org/licenses/by/4.0/>.

© The Author(s) 2026

¹FinnBrain Birth Cohort Study, Turku Brain and Mind Center, Department of Clinical Medicine, University of Turku and Turku University Hospital, Turku, Finland. ²Centre for Population Health Research, Turku University Hospital and University of Turku, Turku, Finland. ³Department of Forensic and Neurodevelopmental Sciences, Institute of Psychiatry, Psychology & Neuroscience, King's College London, London, UK. ⁴Early Life Imaging Research Department, School of Biomedical Engineering and Imaging Sciences, King's College London, London, UK. ⁵Department of Pediatric Neurology, Turku University Hospital, Turku, Finland. ⁶Department of Psychology and Speech-Language Pathology, University of Turku, Turku, Finland. ⁷Department of Teacher Education, University of Turku, Turku, Finland. ⁸Department of Child Psychiatry, University of Turku and Turku University Hospital, Turku, Finland. ⁹Department of Clinical Medicine, Unit of Public Health, University of Turku, Turku, Finland. ¹⁰Department of Psychiatry, University of Turku and Turku University Hospital, Turku, Finland. ¹¹Centre for Eudaimonia and Human Flourishing, Linacre College, University of Oxford, Oxford, UK. ¹²Department of Bioengineering and Institute of Systems and Robotics, LARSyS - Laboratory for Robotics and Engineering Systems, Instituto Superior Tecnico, University of Lisbon, Lisbon, Portugal. ¹³Centre for Music in the Brain, Department of Clinical Medicine, Aarhus University, Aarhus, Denmark. ¹⁴Department of Psychiatry, University of Oxford, Oxford, UK. ¹⁵MRC Centre for Neurodevelopmental Disorders, King's College London, London, UK. ¹⁶Clinical Neurosciences, University of Turku and Turku University Hospital, Turku, Finland. ¹⁷Neurocenter, Turku University Hospital, Turku, Finland. [✉]email: ilmawi@utu.fi